Organic & Biomolecular Chemistry

Cite this: *Org. Biomol. Chem.*, 2012, **10**, 2439

www.rsc.org/obc

PAPER

Syntheses, optical and intramolecular magnetic properties of mono- and di-radicals based on nitronyl-nitroxide and oxoverdazyl groups appended to 2,6-bispyrazolylpyridine cores†

Pramiti Hui, Khaja Md. Arif and Rajadurai Chandrasekar*

Received 8th November 2011, Accepted 6th January 2012
DOI: 10.1039/c2ob06875c

This paper presents the synthesis of a series of nitronyl-nitroxide (NN), oxoverdazyl (OVZ) based mono-, and bi-radicals attached to 4-phenyl-2,6-bispyrazolylpyridine coupling unit, their optical, electron spin resonance (ESR) spectroscopic studies and computational analysis. The ESR studies revealed that the axial zero-field splitting (zfs) parameter of the NN biradical ($|D/hc|$ = 0.00719 cm^{-1}) is larger than the OVZ biradical ($|D/hc|$ = 0.00601 cm^{-1}). Additionally both biradicals displayed forbidden half-field transitions ($\Delta M_s = \pm 2$; $g_{av} \sim 4.01$) at 170 K demonstrating their triplet nature. The cryogenic ESR measurements of the two biradicals showed a Curie magnetic behaviour of the $\Delta M_s = \pm 2$ signal intensities (χ_{EPR}) down to 4.2 K. A detailed comparative analysis of the strength of hyperfine coupling, spin density distribution, zfs and the spin–spin exchange coupling (J) of both NN and OVZ based biradicals showed that the ground state spin multiplicity of both biradicals is probably triplet ($S = 1$) or it is nearly degenerate singlet–triplet states with $J_{NN} \gg J_{OVZ}$.

The design and preparation of paramagnetic molecules is of interest, due to their possible applications in various areas, such as magneto-chemistry,[1,2] bio-organic chemistry,[3] and bio-inorganic chemistry.[4] Among stable radicals, nitroxides (NO), nitronyl-nitroxide (NN) and oxoverdazyl (OVZ) have gained much interest due to their stability, and their propensity to coordinate with d and f block elements. These stable radical units (one or more) attached to chelating ligand cores[5,6] are very attractive since the resultant paramagnetic or high-spin ligands might show interesting magnetic properties (*spin–spin exchange coupling* (J)[1–6]/or *spin cross-over effect*[7]) upon coordination with paramagnetic transition metal ions. In biradical carrying ligands, before metal coordination, understanding the parameters such as zero-field splitting (zfs), spin density distribution, and the J value is crucial. A clear understanding of these factors[4d] requires a comparative ESR spectroscopy investigation of two different classes of *meta* bridged biradicals[8] connected to the same coupling units or spacers. In this context, we designed and synthesized a series of paramagnetic ligands carrying NN and OVZ based mono and biradicals units (**1–6**) connected to 4-phenyl-2,6-bispyrazolylpyridine (bpp) coupling unit (Chart 1). These

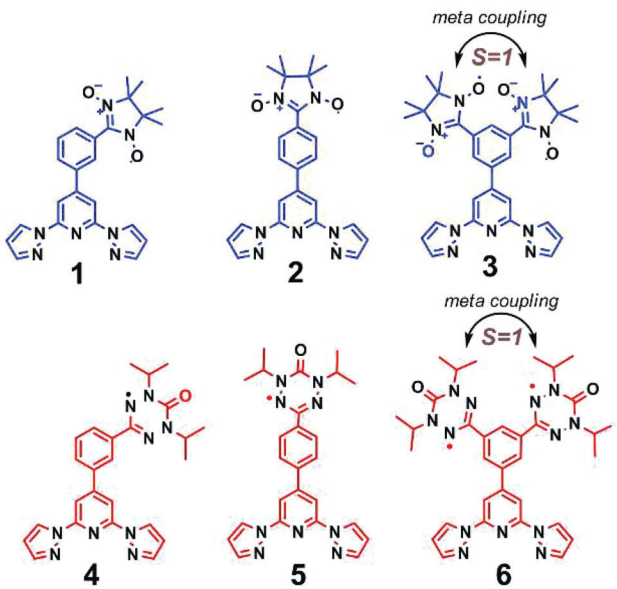

Chart 1 Nitronyl-nitroixde (NN) and oxoverdazyl (OVZ) based mono and di-radicals decorated to 2,6-bispyrazolylpyrines (**1–6**).

radicals also include two *m*-phenylene bridging type NN and OVZ based biradicals (**3** and **6**), leading to non-Kekulé structures for high-spin ground-state formation.[8]

In this paper we report the preparation of mono and biradicals, (**1–6**) their optical and ESR spectroscopy investigations. Single crystal X-ray structure of radical **1** is also presented. A detailed

School of Chemistry, University of Hyderabad, Prof. C. R. Rao Road, Gachi Bowli, Hyderabad – 500 046, India. E-mail: rcsc@uohyd.ernet.in, chandrasekar100@yahoo.com; Fax: +91(40)23134824; Tel: +91 (40)23134824

† Electronic supplementary information (ESI) available: General experimental methods, synthesis, characterization data and spin density calculation. CCDC reference numbers 768145. For ESI and crystallographic data in CIF or other electronic format see DOI: 10.1039/c2ob06875c

analysis to unravel the intramolecular magnetic properties, *i.e.* the interplay between spin polarization, dipolar coupling strengths and the ground-state spin properties also will be presented.

It is important to mention here that the synthesis of NN radicals is not straightforward. The traditional Ullman condensation route,[9] has a series of limitations *i.e.* the reaction of an aryl or alkyl aldehyde group with 2,3-dimethyl-2,3-bis-(hydroxylamino) butane (BHA) followed by oxidation of the diamagnetic condensation product to get NN radicals. Here the synthesis of BHA from 2,3-dimethyl-2,3-bis-(nitro)butane is very sensitive to reaction conditions, such as the quality and particle size of the zinc dust used in the reduction reaction. In most cases the synthesis is very delicate and often not reproducible. Alternatively, a decade ago, Ovcharenko and Rey *et al.* have developed an elegant "*diamino route*" for the synthesis of NN radicals by the condensation reaction of 2,3-dimethyl-2,3-dinitrobutane with aryl-aldehydes bypassing the preparation of BHA.[10] Based on this alternative procedure we have synthesized 2,3-dimethyl-2,3-diaminobutane by reducing 2,3-dimethyl-2,3-dinitrobutane using tin metal under acidic reflux conditions.

The main precursors for the syntheses (Scheme 1) of NN and OVZ based mono and biradicals (**1–6**) are the mono- and di-aldehyde functionalized bpp (**7–9**), respectively. We have prepared compounds **7–9** under Suzuki cross-coupling conditions by reacting 4′-iodo-2′,6′-dipyrazolyl-pyridines[7e] with the corresponding boronic acid derivative of mono or dialdehydes in modest yields of *ca.* 55%. The five-member imidazolidine ring derivatives (**10–12**) were prepared by reacting the aldehyde precursor (**7–9**) with 2,3-dimethyl-2,3-diaminobutane at 60 °C under an inert atmosphere in very good yields. The formation of the five-member imidazolidine moiety is evident from the ^{1}H-NMR chemical shifts of the proton attached to tertiary carbon (N–C*H*–N) typically in the range of 5.27–5.30 ppm (Fig. 1 for **12**). Furthermore LC-MS analyses also confirmed the formation of a five-member imidazolidine ring by displaying *m/z* peaks at 414 for **10** and **11** and 541 for **12**. Finally the introduction of a 1,3-diol in the five-member imidazolidine moiety was effected by treatment of compounds (**10–12**) with *m*-CPBA followed by oxidation with $NaIO_4$ under phase transfer conditions (DCM–water) to get blue coloured NN radicals (**1–3**) in decent yields. The R_f values of radicals **1–3** in acetone–hexane (1 : 9) are 0.17, 0.11, and 0.30, respectively. Radical **1** was crystallized in toluene for single crystal X-ray analysis.

The OVZ-based mono (**4** and **5**) and *m*-phenylene type diradicals (**6**) were also prepared from **7–9**. We employed Brook *et al.*'s procedure to synthesize *N,N*′-diisopropyl substituted OVZ radicals (**4–6**).[2h] It gives OVZ higher stability compared to its *N,N*′-dimethyl substituted analogs. Reaction of 1 equiv of 2,4-diisopropylcarbono-hydrazide bis-hydrochloride with the appropriate aldehyde precursors in reflux ethanol afforded the mono (**13** and **14**) and bistetrazanes (**15**). The ^{1}H-NMR spectra confirmed the formation of tetrazane six-member rings in **13–15** by displaying characteristic chemical shifts in the range of 5.23–5.3 ppm (Fig. 1 for **15**). The tetrazenes were finally oxidized with benzoquinone under reflux condition to get brown-red colour mono (**4** and **5**) and dioxoverdazyl (**6**) radicals. The LC-MS analyses further established the formation of radicals by exhibiting *m/z* peaks at 469 for **4** and **5**, and 649 for **6**. The R_f values of radicals **4–6** in CH_2Cl_2–EtOAc (9 : 1) are 0.58, 0.64, and 0.77, respectively.

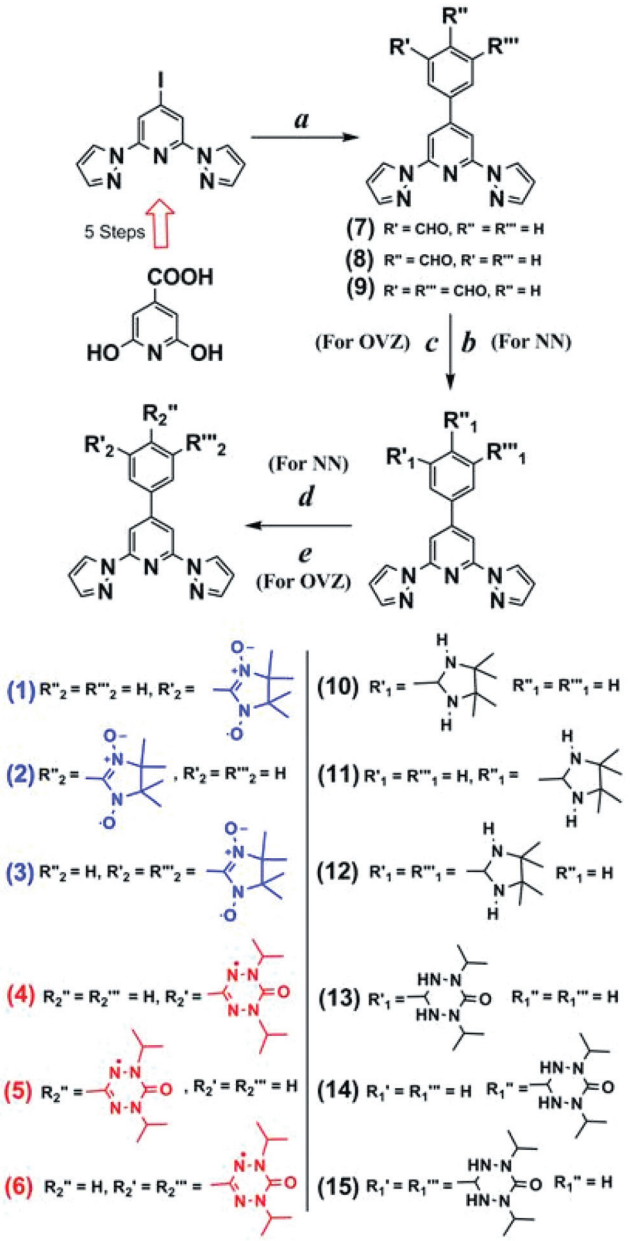

Scheme 1 Synthetic route to nitronyl-nitroixde (NN) and oxoverdazyl (OVZ) based mono- and di-radicals attached to 2,6-bispyrazolylpyrines (**1–6**). *Reagents and conditions:* (a) 3-formylphenyl-boronic acid (for **7**), 4-formylphenyl-boronic acid (for **8**), 3,5-di-formylphenyl-boronic acid (for **9**), $Pd(PPh_3)_4$–1,4-dioxane–Na_2CO_3/3d/70 °C; (*b*) 2,3-diamino-2,3-dimethylbutane–$CHCl_3$/2d/60 °C (*c*) 2,4-diisopropylcarbono-hydrazide bishydrochloride–sodium acetate–EtOH/15 h/RT; (*d*) *m*-CPBA–$NaIO_4$–CH_2Cl_2–H_2O/0 °C/1 h (*e*) benzoquinone–toluene/60 °C

The single crystal X-ray structure of **1** showed that the torsion angles (Φ) between the phenyl ring and the NN radical are 27.60° (C9-C8-C18-N7), and 28.59° (C7-C8-C18-N6) (Fig. 2). Furthermore the phenyl ring and the chelating unit 2,6-bispyrazolylpyridine are in near planar configuration (Φ = *ca.* 24°). The UV-Vis absorption studies of NN radicals (**1–3**) in toluene showed characteristic bands for the n–π* transition in the visible

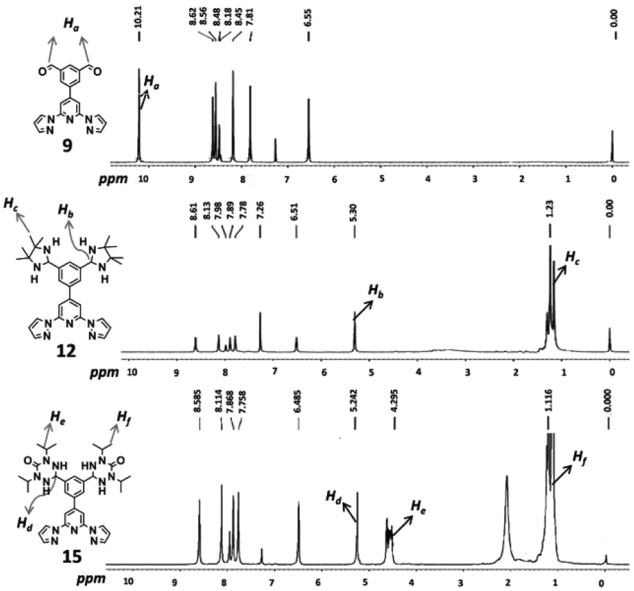

Fig. 1 Comparative ^{1}H-NMR spectra of radical precursors **12** and **15** obtained from dialdehyde **9**.

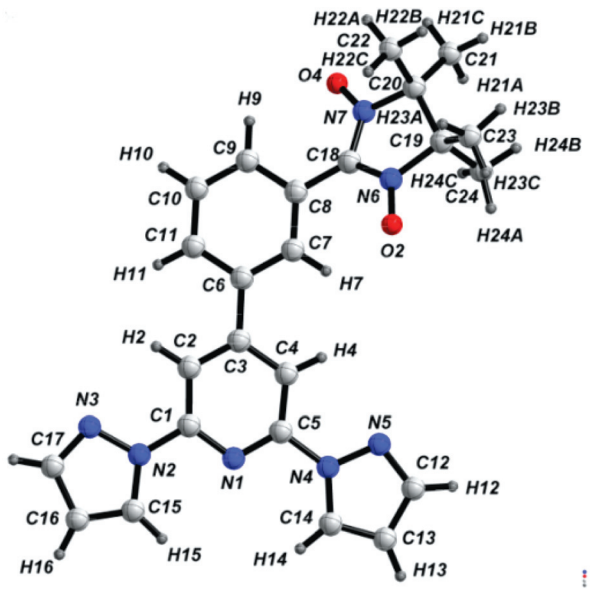

Fig. 2 ORTEP plot (50% probability ellipsoid) of NN radical **1**.

range (λ_{max} ~ 600 nm) with very low extinction coefficient together with the vibronic components (Fig. 3). The electronic absorption spectra of OVZ radicals (**4–6**) displayed distinctive features corresponding to verdazyl radicals. Radicals **4–6** displayed high energy bands at 360, 367 and 374 nm, respectively together with broad low energy bands from 400–650 nm range.

X-band ESR spectroscopy studies of radicals **1–6** were carried out in degassed toluene solution to understand the intramolecular magnetic properties (Fig. 4 and 5; and ESI Fig. S1 and S2†). The room temperature spectra of mono radicals (**1** and **2**) (c ~ 10^{-4} M) exhibited typical five-line pattern ($\Delta M_s = \pm 1$; intensity ratio of 1 : 2 : 3 : 2 : 1) of an NN radical due to the hyperfine coupling (hfc) of the NN electron spin with two equivalent

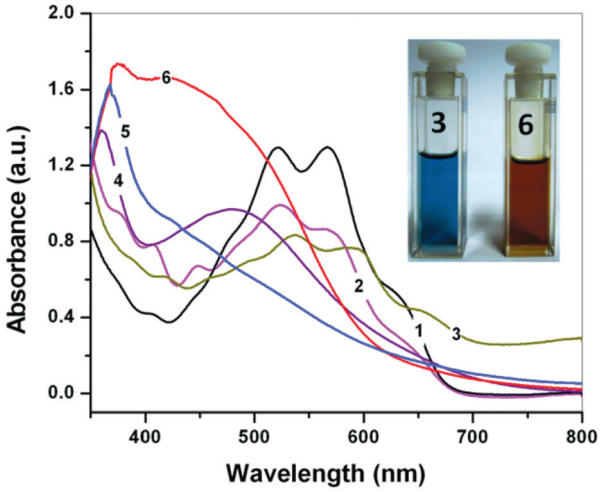

Fig. 3 UV-Vis spectra of NN and OVZ radicals (**1–6**) in toluene. Inset shows the characteristic colour of the biradicals **3** and **6**.

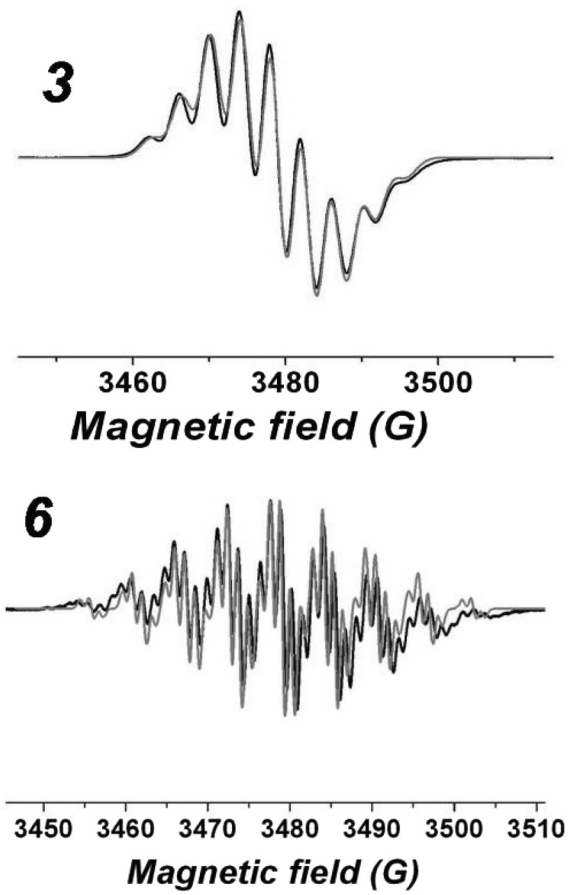

Fig. 4 Isotropic ESR spectra of biradicals **3** and **6** in toluene (c ~ 10^{-4} M) recorded at room temperature. The black and gray lines show the experimental and simulated spectra, respectively.

nitrogen (^{14}N) nuclei. Whereas the spectrum of biradical **3** (c ~ 10^{-4} M) showed characteristic nine-line pattern ($\Delta M_s = \pm 1$; intensity ratio close to 1 : 4 : 10 : 16 : 19 : 16 : 10 : 4 : 1) due to the hfc of the two electron spins with four equivalent nitrogen

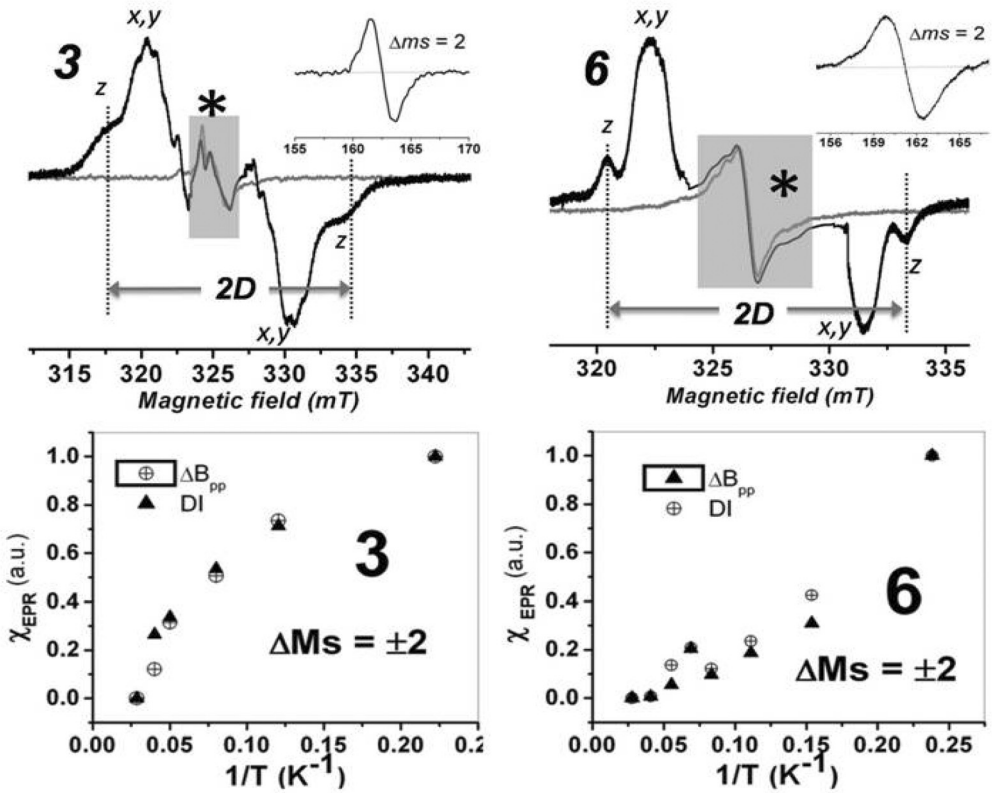

Fig. 5 Top: Electron spin resonance (X-band) frozen state ZFS spectra of biradicals **3** and **6** at 170 K are shown in black lines. The asterix (*) marks and gray shaded regions denote the contribution of the monoradical impurity in **3** and **6**. For comparison the monoradical spectra of **1** and **4** are plotted in gray lines together with the spectra of **3** and **6**, respectively. The inset show the forbidden $\Delta M_s = \pm 2$ transitions. Bottom: Temperature dependence (36–4.2 K) of the doubly integrated signal intensities (χ_{EPR}) and the peak-to-peak signal intensities (ΔB_{pp}) of the $\Delta M_s = \pm 2$ (Curie plot) transitions of **3** and **6**.

(^{14}N) nuclei. The experimental spectra of **1** and **2** were best simulated[11] with the nitrogen hfc (a_N) values of 7.40 G and 7.41 G, respectively. For the case of biradical **3**, due to the strong spin–spin exchange coupling ($2J$) within the EPR limits, the simulation perfectly fits by assuming four nitrogens with half the monoradical hyperfine coupling with $2J \gg 7 \times 10^{-4}$ cm^{-1} ($2J/a_N \gg 1$). The estimated isotropic g-values of radicals **1–3** are 2.0066, 2.0065 and 2.0071, respectively. The room temperature spectra of both mono radicals (**4** and **5**) showed distinct nine-line ($\Delta M_s = \pm 1$ transitions) pattern of an OVZ radical. Additionally, each of the nine lines is composed of a group of lines due to further hfc with magnetically active nuclei of small spin densities. Simulation of the experimental spectra of OVZ radicals (**4** and **5**) showed the following hfc values: a_{N1} = 6.41 G, a_{N2} = 5.35 G and a_H = 1.13 G for **4**; and a_{N1} = 6.20 G, a_{N2} = 5.20 G and a_H = 1.13G for **5**. Interestingly, the spectrum of biradical **6** only exhibited nine-line patterns with an intensity ratio analogous to mono OVZ radical. To our surprise a few literatures which reported the ground state spin multiplicity of OVZ biradicals did not disclose their isotropic hfc pattern.[2f,g] In our case, the obtained nine-line spectrum of biradical **6** demonstrated that the spin–spin exchange coupling between the two radical centres must be close to zero. From the simulation the estimated isotropic g-values of radicals **4–6** are 2.0063, 2.0065 and 2.0071, respectively.

The triplet nature of biradical **3** was clearly apparent from its axial zfs pattern (in toluene; $c \sim 10^{-4}$ M; 170 K) with an unusual resolution of nitrogen hyperfine coupling (Fig. 5 top left). The measured zfs parameter ($2D$) value of **3** is 15.4 mT ($|D/hc|$ = 0.00719 cm^{-1}). By applying a point-dipole approximation, from the experimental D value, the estimated distance between the two NN centres in **3** is *ca.* 7.12 Å. Interestingly, biradical **6** also displayed an axial zfs pattern at 170 K with a $2D$ value of 12.86 mT ($|D/hc|$ = 0.00601 cm^{-1}) proving its biradical nature (Fig. 5 top right). From the D value, an intra-spin distance of separation (r) of *ca.* 7.56 Å was estimated between the two OVZ radical centres in **6**. For comparison the corresponding frozen state monoradical spectra of **1** and **4** are plotted together with the zfs spectra of biradicals **3** and **6**, respectively (see gray lines in Fig. 5).

Furthermore the triplet nature of both NN and OVZ biradicals (**3** and **6**) were clearly supported by the forbidden half-field transitions ($\Delta M_s = \pm 2$; $g_{av} \sim 4.01$) recorded at 170 K (See Fig. 5; top insets). Additionally, the temperature dependency of the $\Delta M_s = \pm 2$ transitions signal intensities of **3** and **6** was followed down to 4.2 K. The measurements were carefully done at lower microwave powers in order to ensure that the signals were not saturated. The plot of the doubly integrated (DI) and of the peak-to-peak (ΔB_{pp}) signal intensities (EPR magnetic susceptibility; χ_{EPR}) of $\Delta M_s = \pm 2$ transitions as function of inverse temperature

(Fig. 5) of **3** and **6** showed sharp increase in the χ_{EPR} value while approaching cryogenic temperature. This behaviour clearly suggested that the triplet state spin population increases with the decrease of temperature by following the Curie pattern. Moreover this finding indicated that the ground-state spin multiplicity is probably triplet ($S = 1$) or the triplet state is nearly degenerate with the singlet state ($S = 0$) for biradicals (**3** and **6**). But it is clear from the obtained hfc pattern that the J value of **3** is definitely much higher than that of **6**, hinting that the two NN radical centres in biradical **3** are more strongly spin–spin exchange coupled than the two OVZ radical centres in biradical **6**.

Additionally, computational studies (DFT; B3LYP) were performed to determine the spin density distribution pattern in biradicals **3** and **6** (ESI Fig. S3†). The value of spin density (ρ^C) distributions in NN nodal plane carbon ($\rho^C_{NN} = -0.2057$) and next phenyl coupler carbon ($\rho^C_{Ph} = 0.0521$) in biradical **3** are larger than the OVZ nodal plane carbon ($\rho^C_{OVZ} = -0.129$) and next phenyl coupler carbon ($\rho^C_{Ph} = 0.0340$). But the comparison of the torsion angles (Φ) between the phenyl ring and the radical plane showed that they are more planar [Φ is *ca.* 15°][2h] in biradical **6** than that of **3** [Φ = *ca.* 28°] (for **3** radical **1** in Fig. 2). This data suggested that the electronic structure of the five-member NN ring favours more spin density leakage to the coupling unit compared to the six-member OVZ ring (more delocalization inside the ring). This observation was further supported by the different D values obtained for biradicals **3** and **6** in the low temperature EPR measurements.

Conclusions

Recently, Eaton, Neese *et al.*[4d] have reported that at shorter spin distances or in delocalized spin systems the use of point-dipole approximation is inadequate (*i.e.*, *deviation from* R^{-3} *behaviour*). Most of the time the intra-radical distance derived from the experimental zfs is inconsistent with the X-ray structure. Moreover the spin–spin contribution to the zfs parameter dictates the zfs when $S \geq 1$. In our present case, to study the relative difference in the D values, two types (NN and OVZ) of biradicals connected to the same 4-pheny-2,6-bispyrazolylpyridine coupling unit (**3** and **6**) were synthesized. The obtained difference in the D and r (*calculated via point-dipole approximation*) values between the two types of biradicals attached to the same unsaturated molecular backbone (**3** and **6**) are 0.00118 cm^{-1} and *ca.* 0.44 Å, respectively. The significant difference observed in the D values of **3** and **6** clearly confirmed the existing variations in the orientation of the two spin carrying units, their spin density distributions and the resulting dipolar coupling strengths. From the computational studies it is clear that in **3** the spin density wave is more delocalized into the whole molecular backbone there by reducing the average r value between the two spins (larger D value) compared to biradical **6** (smaller D value). Additionally since the amount of spin density wave propagation is also related to the spin–spin exchange interaction (J), the obtained results demonstrated that the NN biradicals in **3** are rather more strongly exchange coupled than the OVZ biradicals in **6** *i.e.* $J_{NN} \gg J_{OVZ}$.

Experimental section

General methods

3-Formylphenyl-boronic acid, 4-formylphenyl-boronic acid, 3,5-diformylphenyl-boronic acid, pyrazole and citrazinic acid were obtained from Aldrich. Potassium, trifluoro acetic acid, diglyme, and NaIO4 were purchased from Spectrochem Pvt. Ltd, Mumbai. Dichloromethane, hexane, pet-ether, $CHCl_3$, dioxane, toluene and methanol solvents were obtained from Finar Chemicals Limited, Ahmadabad, India. All solvents were used after distillation. CO_2Cl_2, I_2, LiOH, tetramethylammonium chloride, $POCl_3$, mCPBA, anhydrous $MgSO_4$, K_2CO_3, and KI were obtained from Avra Synthesis, Hyderabad, India. Deuterated solvents $CDCl_3$-d_1, and DMSO-d_6 were obtained from Aldrich and Merck respectively. ^1H and ^{13}C NMR spectroscopic data were recorded on a Bruker DPX 400 spectrometer with solvent proton as internal standard ($CDCl_3$-d_1 = 7.26 ppm and DMSO-d_6 = 2.50 ppm). Column chromatography was performed using Merck silica gel (particle size 100–200 mesh). LC mass spectrometry was performed on Shimadzu LCMS-2010A mass spectrometer. IR spectra were recorded on JASCO FT/IR-5300. Elemental analyses were recorded on a Thermo Finnigan Flash EA 1112 analyzer. For thin-layer chromatography (TLC), silica gel plates Merck 60 F254 were used and compounds were visualized by irradiation with UV light. EPR spectra were recorded on a Bruker-ER073 instrument equipped with an EMX microX source for X band measurement using Xenon 1.1b.60 software provided by the manufacturer. For the liquid helium temperature measurements, a temperature controller supplied from Oxford instruments (ITC 503S) was used.

4-(2,6-Di(pyrazol-1-yl)pyridin-4-yl)benzaldehyde (8). In 100 mL flask, 1,4-dioxane (20 mL) and 2 M Na_2CO_3 (5 mL) were taken together and N_2 gas was bubbled through the solution for 30 min. To this 4′-iodo-2′,6′-dipyrazolyl-pyridine (200 mg, 0.593 mmol), 4-formylphenylboronic acid (106 mg, 0.712 mmol), and $Pd(PPh_3)_4$ (43 mg, 0.031 mmol, 5%) were added and heated to 70 °C for 3 d under nitrogen atmosphere. The solvent was removed *in vacuo* and the remaining residue was treated with water and extracted with CH_2Cl_2 (3 × 50 mL). The combined organic layer was dried with $MgSO_4$ and the solvent was removed *in vacuo* to get a light greenish solid residue. This coloured residue was washed with methanol to remove the soluble impurities and to isolate a white colour powder of **8**. Yield: 100 mg (53%). ^1H NMR (400 MHz, $CDCl_3$-d_1, δ_{ppm}) 10.10 (s, 1H, –CHO), 8.61 (d, 2H), 8.13 (d, 2H), 8.03–7.95 (m, 4H), 7.79 (s, 2H), 6.53 (m, 2H) ppm. ^{13}C NMR (100 MHz, $CDCl_3$-d_1, δ_{ppm}) δ 191.6, 152.7, 150.8, 143.2, 142.6, 136.9, 130.4, 128.0, 127.3, 108.2, 107.5 ppm. LCMS analysis (*m/z*): found 316.10; calcd 315.11. FT-IR (KBr): 2963, 2917, 28589, 1703 (–CHO), 1620, 1557, 1466, 1395, 1262, 1209, 1032, 937, 792 cm^{-1}. Anal. calcd for $C_{18}H_{13}N_5O$ (315.11): found C, 68.65; N, 22.45; H 4.09%; requires C, 68.56; N, 22.21; H, 4.16%.

3-(2,6-Di(pyrazol-1-yl)pyridin-4-yl)benzaldehyde (7). *Similar procedure for the synthesis of* **8** *was applied*. 4′-Iodo-2′,6′-dipyrazolylpyridine (200 mg, 0.5932 mmol), 3-formylphenyl-boronic acid (106 mg, 0.712 mmol), 2 M Na_2CO_3 (5 mL) and $Pd(PPh_3)_4$

(43 mg, 0.031 mmol, 5%). White colour powder of **7**. Yield: 92 mg (51%) ^{1}H NMR (400 MHz, $CDCl_3$-d_1, δ_{ppm}): 10.13 (s, 1H, –CHO), 8.62–8.61 (d, 2H), 8.32 (t, 1H), 8.15 (s, 2H), 8.10–8.08 (m, 1H), 8.01 (m, 1H), 7.8 (d, 2H), 7.71–7.67 (t, 1H), 6.54–6.53 (q, 2H). ^{13}CNMR (100 MHz, $CDCl_3$-d_1, δ_{ppm}): 191.7, 152.7, 150.8, 142.6, 138.5, 137.2, 133.0, 130.5, 129.9, 128.6, 127.3, 108.2, 107.3. LCMS analysis (*m/z*): found 316.10; calcd 315.11. FT-IR (KBr): 3432, 2963, 1699 (–CHO), 1618, 1562, 1522, 1470, 1399, 1262, 1036, 949, 862, 799, 540 cm^{-1}. Anal. calcd for $C_{18}H_{13}N_5O$ (315.11): found C 68.65, N 22.45, H 4.09%; requires C 68.56, N 22.21, H 4.16%.

5-(2,6-Di(pyrazol-1-yl)pyridin-4-yl)isophthalaldehyde (9). *Similar procedure for the synthesis of* **8** *was applied.* 4′-Iodo-2′,6′-dipyrazolyl-pyridine (200 mg, 0.59 mmol), 3,5-diformyl-phenylboronic acid (126 mg, 0.712 mmol) and $Pd(PPh_3)_4$ (80 mg, 0.031 mmol, 5%). White colour powder of **9**. Yield: 125 mg (58%). ^{1}H-NMR (400 MHz, $CDCl_3$-d_1, δ_{ppm}): 10.21 (s, 2H, –CHO), 8.62–8.56 (d, 4H), 8.48 (s, 1H), 8.18 (s, 2H), 7.81 (s, 2H), 6.55 (m, 2H). ^{13}C-NMR (100 MHz, $CDCl_3$-d_1, δ_{ppm}) δ: 190.4, 151.3, 151.0, 142.8, 139.8, 137.9, 133.1, 131.2, 127.3, 108.4, 107.2. LCMS analysis (*m/z*): found 344.0; calcd 343.11. FT-IR (KBr): 3403, 2919, 1698(–CHO), 1616, 1464, 1397, 1262, 1020, 801 cm^{-1}. Anal. calcd for $C_{18}H_{13}N_5O$ (541.82): found C, 66.32; N 20.54, H 3.88%; requires C 68.47, N 20.40, H 3.82%.

General procedure for tetrazanes

6-(3-(2,6-Di(pyrazol-1-yl)pyridin-4-yl)phenyl)-2,4-diisopropyl-1,2,4,5-tetrazinan-3-one (13). In a typical procedure, 2,4-diisopropylcarbonohydrazide bishydrochloride (81 mg, 0.468 mmol) and 3-(2,6-di(pyrazol-1-yl)pyridin-4-yl)benzaldehyde (**7**) (100 mg, 0.312 mmol) were dissolved completely in a minimum amount of ethanol (10 mL). To this clear solution was added sodium acetate (51 mg, 0.624 mmol) and the solution was allowed to stir at room temperature for 15 h (no noticeable colour change was found). The turbid solution was filtered to remove the sodium acetate and the filtrate was evaporated *in vacuo* to get a yellowish-white residue. The residue was recrystallized from heptane to get white colour tetrazane compound **13**. Yield: 87 mg (60%). ^{1}H-NMR (400 MHz, $CDCl_3$-d_1, δ_{ppm}): 8.62–8.61 (d, 2H), 8.14 (s, 2H), 8.01 (s, 1H), 7.79–7.72 (m, 4H), 7.51–7.49 (m, 1H), 6.52 (d, 2H), 5.29 (s, 1H, N–C*H*–N), 4.88–4.16 (m, 2H), 1.33–1.13 (m, 12H). ^{13}C-NMR (100 MHz, $CDCl_3$-d_1, δ_{ppm}) δ: 154.4, 150.9, 149.1, 146.5, 142.6, 132.3, 132.2, 131.5, 128.6, 128.5, 127.1, 108.1, 107.8, 63.0, 31.9, 31.4, 31.0, 29.7, 29.4, 25.3, 23.6, 23.0, 22.7, 14.1. LCMS analysis (*m/z*): found 471.30; calcd 471.56. FT-IR (KBr): 2982, 1722, 1647, 1574, 1417, 1255, 1105, 1051, 771, 652, 623, 457 cm^{-1}. Anal. calcd for $C_{25}H_{29}N_5O$ (471.25): found C 63.48, N 26.59, H 6.25%; requires C, 63.68; H, 6.20; N, 26.73%.

6-(4-(2,6-Di(pyrazol-1-yl)pyridin-4-yl)phenyl)-2,4-diisopropyl-1,2,4,5-tetrazinan-3-one(14). *Compound* **14** *was synthesized by above tetrazane procedure.* 2,4-Diisopropylcarbonohydrazide bishydrochloride (81 mg, 0.468 mmol), 4-(2,6-di(pyrazol-1-yl) pyridin-4-yl)benzaldehyde (**8**) (100 mg, 0.312 mmol), and sodium acetate (51 mg, 0.624 mmol). Yield: 93 mg (63%).^{1}H-NMR (400 MHz, $CDCl_3$-d_1, δ_{ppm}): 8.62 (s, 2H), 8.14 (s, 1H), 8.01 (s, 1H), 7.79–7.72 (m, 6H), 6.55 (s, 2H), 5.30 (s, 1H, N–C**H**–N), 4.30–4.12 (m, 2H), 1.33–1.13 (m, 12H). ^{13}C-NMR (100 MHz, $CDCl_3$-d_1, δ_{ppm}) δ: 154.4, 150.6, 142.3, 137.5, 129.2, 127.6, 127.2, 126.5, 125.5, 107.9, 107.4, 62.1, 31.9, 31.4, 31.0, 29.7, 29.4, 25.3, 23.6, 23.0, 22.7, 14.1. LCMS analysis (*m/z*) found 472.00; calcd 471.56. FT-IR (KBr): 3435.5, 3288.9, 3165.5, 2999.6, 1701.4, 1641.6, 1566.3, 1413.9, 1049.4, 1012.7, 923.99, 810.2, 650.1, 623.1, 522.8, 464.9 cm^{-1}. Anal. calcd for $C_{25}H_{29}N_5O$ (471.25): found C, 63.58; N, 26.45; H, 6.25; requires, 63.68; H, 6.20; N, 26.73%.

6,6′-(5-(2,6-Di(pyrazol-1-yl)pyridin-4-yl)-1,3-phenylene)bis(2,4-diisopropyl-1,2,4,5-tetrazinan-3 one) (15). *Compound* **15** *also synthesized by same procedure*. 2,4-Diisopropylcarbonohydrazide bishydrochloride (152 mg, 0.87 mmol), 5-(2,6-di(pyrazol-1-yl)pyridin-4-yl)isophthalaldehyde (**9**) (100 mg, 0.343 mmol), and sodium acetate (72 mg, 0.87 mmol). Yield: 111 mg (59%). ^{1}H-NMR (400 MHz, $CDCl_3$-d_1, δ_{ppm}): 8.58 (s, 2H), 8.11 (s, 2H), 7.86 (s, 1H), 7.75 (m, 4H), 6.48 (s, 2H), 5.24 (s, 2H, N–C*H*–N), 4.88–4.13 (m, 4H), 1.23–1.05 (m, 24H). ^{13}C-NMR (100 MHz, $CDCl_3$-d_1, δ_{ppm}) δ: 154.0, 150.6, 149.9, 147.1, 145.8, 142.7, 136.5, 127.2, 107.9, 107.4, 63.6, 31.9, 31.4, 31.0, 29.7, 29.4, 25.3, 23.6, 23.0, 22.7, 14.2. LCMS analysis (*m/z*): found 655.60; calcd 655.80. Anal. calcd for $C_{33}H_{45}N_{13}O_2$ (655.80): found C, 60.58; N, 27.45; H, 6.85%; requires, C, 60.44; H, 6.92; N, 27.77%; FT-IR (KBr): 3435.5, 3288.9, 2980.3, 2935.9, 2878.1, 1738.0, 1707.2, 1641.6, 1564.4, 1412.0, 1250, 1155.5, 1045.5, 1012.7, 920.1, 852.6, 788.9, 646.2, 530.5 cm^{-1}.

General procedure for 4,4,5,5-tetramethylimidazolidines

2,6-Di(pyrazol-1-yl)-4-(4-(4,4,5,5-tetramethylimidazolidin-2-yl)phenyl)pyridine (11). In a typical procedure, a solution of 4–2,6-di(pyrazol-1-yl)pyridin-4-yl-benzaldehyde (**8**) (200 mg, 0.634 mmol) in chloroform (10 mL) was added drop-wise to a solution of 2,3-diamino-2,3-dimethylbutane (110 mg, 0.952 mmol) in chloroform (20 mL) in a round bottom flask. The reaction mixture was heated at 60 °C for 2 d under argon to get a light turbid solution. The TLC confirmed the complete consumption of **8** (R_f = 0.55; 3 : 2 DCM–hexane). The solution was directly dried with Na_2SO_4 and evaporated *in vacuo* to get compound **11** as a white powder. Yield: 172 mg (66%). ^{1}H-NMR (400 MHz, $CDCl_3$-d_1, δ_{ppm}): 8.63 (s, 2H), 8.18 (s, 2H), 7.84, 7.82, 7.8, 7.73, 6.53 (s, 2H), 5.27 (s, 1H, N–C*H*–N), 1.25, 1.23, 1.13. ^{13}C-NMR (100 MHz, $CDCl_3$-d_1, δ_{ppm}): 153.9, 150.6, 145.8, 142.4, 136.5, 127.2, 108.0, 107.2, 73.0, 63.0, 31.0, 25.3, 23.6, 14.2. LCMS analysis (*m/z*): found, 414.25; calcd, 413.52. FT-IR (KBr): 3335, 2978, 2919, 2855, 1615, 1541, 1460, 1391, 1273, 1171, 694 cm^{-1}. Anal. Calcd for $C_{18}H_{13}N_5O$ (541.82): found C 69.58, N 23.85, H 6.51. Required C, 69.71; H, 6.58; N, 23.71.

2,6-Di(pyrazol-1-yl)-4-(3-(4,4,5,5-tetramethylimidazolidin-2-yl)phenyl)pyridine(10). *Compound* **10** *was synthesized by above condensation procedure*. 3-(2,6-Di(pyrazol-1-yl)pyridin-4-yl) benzaldehyde (**7**) (200 mg, 0.634 mmol) and 2,3-diamino-2,3-dimethylbutane (110 mg, 0.952 mmol) Yield: 163 mg (62%);

^{1}H-NMR (400 MHz, $CDCl_3$-d_1, δ_{ppm}): 8.62 (s, 2H), 8.14 (s, 2H), 8.01 (s, 1H), 7.79–7.74 (m, 4H), 7.72 (s, 1H), 6.52 (s, 2H), 5.30 (s, 1H, N–C*H*–N), 1.34–1.14 (s, 12H). ^{13}C-NMR (100 MHz, $CDCl_3$-d_1, δ_{ppm}): 154.4, 150.6, 145.2, 144.0, 142.3, 140.5, 139.0, 137.5, 129.2, 127.6, 127.2, 126.5, 125.5, 108.0, 107.5, 97.2, 87.3, 73.1, 63.0, 31.5, 31.0, 25.3, 24.0, 23.1, 14.1. LCMS analysis (*m/z*): found, 413.65; calcd, 413.52. FT-IR (KBr): 3335, 2978, 2919, 2855, 1615, 1541, 1460, 1391, 1273, 1171, 694 cm^{-1}. Anal. Calcd for $C_{18}H_{13}N_5O$ (541.82): found C 69.58, N 23.85, H 6.51. Required C, 69.71; H, 6.58; N, 23.71.

4-(3,5-Bis(4,4,5,5-tetramethylimidazolidin-2-yl)phenyl)-2,6-di (1H-pyrazol-1-yl)pyridine (12). *Compound* (**12**) *was synthesized by above condensation procedure*. 5-(2,6-Di(pyrazol-1-yl) pyridin-4-yl)isophthalaldehyde (**9**) (200 mg, 0.583 mmol) and 2,3-diamino-2,3-dimethylbutane (192 mg, 1.748 mmol). Yield: 172 mg (55%). ^{1}H-NMR (400 MHz, $CDCl_3$-d_1, δ_{ppm}): 8.61 (s, 2H), 8.13 (s, 2H), 7.99 (s, 1H), 7.90 (s, 2H), 7.77 (s, 2H), 6.52 (s, 2H), 5.30 (s, 2H, N–C*H*–N), 1.30–1.16 (m, 24H). ^{13}C-NMR (100 MHz, $CDCl_3$-d_1, δ_{ppm}): 154.5, 150.6, 142.3, 137.7, 127.2, 125.7, 125.1, 108.0, 73.4, 63.3, 25.4, 24.5, 23.6. LCMS analysis (*m/z*): found, 540.8; calcd, 539.35. FT-IR (KBr): 3337, 2969, 2932, 2855, 1721, 1617, 1561, 1466, 1397, 1208, 1169, 1042, 938, 862, 758 cm^{-1}.

General procedure for NN radicals

2,6-Di(pyrazol-1-yl)-4-(3-(1-oxy-3oxo-4,4,5,5-tetramethylimidazolidin-2-yl)phenyl)pyridine (1). A solution of *m*-chloroperbenzoic acid (84 mg, 0.145 mmol) in methylene chloride (5 mL) was added drop-wise to a mixture containing **10** (20 mg, 0.048 mmol) and saturated solution of $NaHCO_3$ (1 mL) in an ice bath and stirred for one hour. A light blue tint was slowly developed indicating the formation of a nitronyl-nitroxide radical. To this solution, $NaIO_4$ (21 mg, 0.0968 mmol) in water (10 mL) was added drop-wise and then stirred for 30 min to get a dark blue colour solution, which indicated the complete oxidization of the radical precursor. From the phase transfer solution, the dark blue organic layer was separated, and the light blue aqueous layer was twice extracted with dichloromethane (20 mL × 2). The organic layers were combined and dried with $MgSO_4$ and the solvent was evaporated *in vacuo* to get radical **1** as a blue solid. Yield: 6 mg (30%). R_f = 0.17 (10% acetone–hexane). EPR (in toluene; $c \sim 10^{-4}$ M, RT, ν = 9.13782 GHz, 0.998 mW power, 1 scan): five lines, g_{iso} = 2.0066, a_N = 7.41 G. UV-Vis (in toluene $c = 5 \times 10^{-3}$ M): λ_{abs} (ε) 567 nm (1296 M^{-1} cm^{-1}), 300 nm (ε = 6970 M^{-1} cm^{-1}). FT-IR (KBr): 3253, 2982, 2931, 1734, 1654, 1526, 1464, 1390, 1265, 1224, 1188, 945, 834, 831, 749, 680, 567, 443 cm^{-1}.

2,6-Di(pyrazol-1-yl)-4-(4-(1-oxy-3oxo-4,4,5,5-tetramethylimidazolidin-2-yl)phenyl)pyridine (2). *m*-Chloroperbenzoic acid (84 mg, 0.145 mmol), 2,6-di(pyrazol-1-yl)-4-(4-(4,4,5,5-tetramethylimidazolidin-2-yl)phenyl)pyridine (**11**) (20 mg, 0.048 mmol) and $NaIO_4$ (21 mg, 0.0968 mmol) Yield: 7 mg (35%). R_f = 0.11 (10% acetone–hexane). EPR (in toluene $c \sim 10^{-4}$ M, RT, ν = 9.14166 GHz, 0.998 mW power, 1 scan): five lines, g_{iso} = 2.0067, a_N = 7.40 G. UV-Vis (in toluene $c = 5 \times 10^{-3}$ M): λ_{abs} (ε) 537 nm (667 M^{-1} cm^{-1}), 314 nm (1482 M^{-1} cm^{-1}). FT-IR (KBr): 3233, 2982, 2922, 1754, 1654, 1556, 1464, 1391 (N–O), 1262, 1221, 1088, 945, 874, 831, 749, 651, 517, 440 cm^{-1}.

4-(3,5-Bis(1-oxy-3oxo-4,4,5,5-tetramethylimidazolidin-2-yl) phenyl)-2,6-di(1H-pyrazol-1-yl)pyridine (3). *m*-Chloroperbenzoic acid (168 mg, 3.336 mmol), 4-(3,5-bis(4,4,5,5-tetramethylimidazolidin-2-yl)phenyl)-2,6-di(1H-pyrazol-1-yl)pyridine (**12**) (30 mg, 0.556 mmol) and $NaIO_4$ (23 mg, 1.112 mmol) Yield: 4 mg (20%). R_f = 0.30 (10% acetone–hexane). EPR (in toluene $c \sim 10^{-4}$ M, RT, ν = 9.13829 GHz, 0.998 mW power, 1 scan): nine lines, g_{iso} = 2.0071. UV-Vis (in toluene $c = 5 \times 10^{-3}$ M): λ_{abs} (ε) 592 nm (524 M^{-1} cm^{-1}), 303 nm (2007 M^{-1} cm^{-1}). FT-IR (KBr): 2924, 2854, 1734, 1616, 1560, 1521, 1466, 1394, 1261, 1124, 1039, 952, 862, 788, 540 cm^{-1}. EPR (in toluene $c \sim 10^{-4}$ M, ν = 9.14572 GHz, 0.998 mW power, 1 scan): g_{iso} = 2.0071, $|D/hc|$ = 0.00719 cm^{-1}, $\Delta M_s = \pm 2$ transition $g_{av} \sim 4.01$. Anal. calcd for $C_{31}H_{35}N_9O_4$ (597.67): N, 21.09; found C, 62.15; H, 5.95; N, 21.32; requires C, 62.30; H, 5.90.

General procedure for OVZ radicals

6-(3-(2,6-Di(pyrazol-1-yl)pyridin-4-yl)phenyl)-2,4-diisopropyl -3-oxoverdazyl (4). In a typical procedure, 6-(3-(2,6-di(pyrazol-1-yl)pyridin-4-yl)phenyl)-2,4-diisopropyl-1,2,4,5-tetrazinan-3-one (**13**) (100 mg, 0.212 mmol) was heated with benzoquinone (34 mg, 0.318 mmol) in 5 mL toluene at 40 °C for 30 min. When TLC indicated that the starting material had disappeared the resulting solution was cooled, filtered and evaporated. Chromatography of the residue on silica gel using CH_2Cl_2–EtOAc (9 : 1) gave a brown solid of **4**. Yield: 25 mg (24%). R_f = 0.58 in CH_2Cl_2–EtOAc (9 : 1). LCMS analysis calcd (*m/z*): 468.53, found 468.4. UV-Vis (in toluene): λ_{abs} 360 and 374 nm. FT-IR (KBr): 3243, 2984, 2932, 1734, 1634, 1516, 1464, 1373, 1262, 1221, 1088, 945, 874, 831, 760, 681, 527, 448 cm^{-1}. EPR (in toluene $c \sim 10^{-4}$ M, RT, ν = 9.14577 GHz, 0.998 mW power, 1 scan): nine lines, g_{iso} = 2.0063, a_{N1} = 6.41 G, a_{N2} = 5.35G and a_H = 1.13G. Anal. calcd for $C_{25}H_{26}N_9O$ (468.53): found C, 64.17; H, 5.48; N, 26.88; requires C, 64.09; H, 5.59; N, 26.91.

6-(4-(2,6-Di(pyrazol-1-yl)pyridin-4-yl)phenyl)-2,4-diisopropyl-3-oxoverdazyl (5). *Compound* (**5**) *was synthesized by following the above procedure.* 6-(4-(2,6-Di(pyrazol-1-yl)pyridin-4-yl) phenyl)-2,4-diisopropyl-1,2,4,5-tetrazinan-3-one (**14**) (100 mg, 0.212 mmol) and benzoquinone (34 mg, 0.318 mmol) Yield: 27 mg (26%). R_f = 0.64 in CH_2Cl_2–EtOAc (9 : 1). LCMS analysis (*m/z*): calcd 468.53; found 469.05. UV-Vis (in toluene): λ_{abs} 400–650 nm. FT-IR (KBr): 3243, 2984, 2932, 1734, 1634, 1516, 1464, 1373, 1262, 1221, 1088, 945, 874, 831, 760, 681, 527, 448 cm^{-1}. EPR (in toluene $c \sim 10^{-4}$ M, RT, ν = 9.14808 GHz, 0.998 mW power, 1 scan): nine lines, g_{iso} = 2.0063, a_{N1} = 6.20 G, a_{N2} = 5.20 G and a_H = 1.13G. Anal. calcd for $C_{25}H_{26}N_9O$ (468.53): found C 64.15, N 26.78, H 5.48; requires C, 64.09; H, 5.59; N, 26.91.

6-(3,5-(2,6-Di(pyrazol-1-yl)pyridin-4-yl)phenyl)-2,4-diisopropyl-3-oxoverdazyl (6). *Compound* (**6**) *was synthesized by following the above procedure.* 6,6′-(5-(2,6-Di(pyrazol-1-yl)pyridin-4-yl)-1,3-phenylene)bis(2,4-diisopropyl-1,2,4,5-tetrazinan-3 one)

(**15**) (100 mg, 0.152 mmol) and benzoquinone (49 mg, 0.457 mmol) Yield: 21 mg (20%). R_f = 0.77 in CH_2Cl_2–EtOAc (9 : 1). LCMS analysis (*m/z*): calcd 649.74; found 648.75. UV-Vis (in toluene): λ_{abs} 360 and 480 nm. FT-IR (KBr): 3246, 2982, 2936, 1736, 1634, 1555, 1470, 1370, 1258, 1223, 1101, 949, 874, 831, 762, 679, 527, 448 cm^{-1}. EPR (in toluene $c \sim 10^{-4}$ M, ν = 9.14808 GHz, 0.998 mW power, 1 scan): g_{iso} = 2.0071, $|D/hc|$ = 0.00601 cm^{-1}, $\Delta M_s = \pm 2$ transition with $g_{av} \sim$ 4.01. Anal. calcd for $C_{33}H_{39}N_{13}O_2$ (649.75): found: C 61.22, N 27.86, H 6.16; requires C, 61.00; H, 6.05; N, 28.02.

Acknowledgements

We are grateful to DST (Fast Track Scheme No. SR/FTP/CS-115/2007), New Delhi for financial support. P. H. thanks CSIR for a SRF.

Notes and references

1 (*a*) H. Iwamura and N. Koga, *Acc. Chem. Res.*, 1993, **26**, 346–351; (*b*) A. Rajca, *Chem. Rev.*, 1994, **94**, 871–893; (*c*) *Magnetic Properties of Organic Materials*, ed. P. M. Lahti, Marcel Dekker, New York, 1999, pp. 1–713; (*d*) *Molecular Magnetism*, ed. K. Itoh and M. Kinoshita, Gordon and Breach, Kodansha, 2000, pp. 1–337; (*e*) M. Baumgarten, High spin molecules directed towards molecular magnets, in *EPR of Free Radicals in Solids, Trends in Methods and Application*, ed. A. Lund and M. Shiotani, Kluwer, 2003/2004, ch. 12, pp. 491–528.

2 (*a*) A. Rajca, J. Wongsriratanakul and S. Rajca, *Science*, 2001, **294**, 1503–1505; (*b*) S. Rajca, A. Rajca, J. Wongsriratanakul, P. Butler and S. Choi, *J. Am. Chem. Soc.*, 2004, **126**, 6972–6986; (*c*) A. Rajca, J. Wongsriratanakul and S. Rajca, *J. Am. Chem. Soc.*, 2004, **126**, 6608–6626; (*d*) A. Rajca, J. Wongsriratanakul, S. Rajca and R. L. Cerny, *Chem.–Eur. J.*, 2004, **10**, 3144–3157; (*e*) E. Fukuzaki and H. Nishide, *J. Am. Chem. Soc.*, 2006, **128**, 996–1001; (*f*) D. J. R. Brook and G. T. Yee, *J. Org. Chem.*, 2006, **71**, 4889–4895; (*g*) J. B. Gilroy, S. D. J. McKinnon, P. Kennepohl, M. S. Zsombor, M. J. Ferguson, L. K. Thompson and R. G. Hicks, *J. Org. Chem.*, 2007, **72**, 8062–8069; (*h*) E. C. Parè, D. J. R. Brook, A. Brieger, M. Badik and M. Schinke, *Org. Biomol. Chem.*, 2005, **3**, 4258–4261; (*i*) P. Taylor and P. M. Lahti, *Chem. Commun.*, 2004, 2656; (*j*) Md. E. Ali, S. Vyas and S. N. Datta, *J. Phys. Chem. A*, 2005, **109**, 6272–6278; (*k*) Md. E. Ali and S. N. Datta, *J. Phys. Chem. A*, 2006, **110**, 2776–2784.

3 (*a*) E. J. Hustedt and A. H. Beth, *Annu. Rev. Biophys. Biomol. Struct.*, 1999, **28**, 129–153; (*b*) S. S. Eaton and G. R. Eaton, *Biol. Magn. Reson.*, 2000, **19**, 1–27; (*c*) C. Altenbach, K.-J. Oh, R. Trabanino, K. Hideg and W. Hubbell, *Biochemistry*, 2001, **40**, 15471–15482; (*d*) P. Hanson, G. Millhauser, F. Formaggio, M. Crisma and C. Toniolo, *J. Am. Chem. Soc.*, 1996, **118**, 7618–7625; (*e*) D. Hilger, Ye. Polyhach, E. Padan, H. Jung and G. Jeschke, *Biophys. J.*, 2007, **93**, 3675–3683; (*f*) G. Jeschke, *Biochim. Biophys. Acta, Bioenerg.*, 2005, **1707**, 9–102.

4 (*a*) D. S. Marlin, E. Bill, T. Weyhermüller, E. Bothe and K. Wieghardt, *J. Am. Chem. Soc.*, 2005, **127**, 6095–6108; (*b*) P. Ghosh, E. Bill, T. Weyhermüller and K. Wieghardt, *J. Am. Chem. Soc.*, 2003, **125**, 3967–3979; (*c*) C. Mukherjee, U. Pieper, E. Bothe, V. Bachler, E. Bill, T. Weyhermüller and P. Chaudhuri, *Inorg. Chem.*, 2008, **47**, 8943–8956; (*d*) C. Riplinger, J. P. Y. Kao, G. M. Rosen, V. Kathirvelu, G. R. Eaton, S. S. Eaton, A. Kutateladze and F. Neese, *J. Am. Chem. Soc.*, 2009, **131**, 10092–10106.

5 (*a*) C. Rajadurai, A. Ivanova, V. Enkelmann and M. Baumgarten, *J. Org. Chem.*, 2003, **68**, 9907; (*b*) C. Rajadurai, S. Ostrovsky, K. Falk, V. Enkelmann, W. Haase and M. Baumgarten, *Inorg. Chim. Acta*, 2004, **357**, 581; (*c*) C. Rajadurai, O. Fuhr, V. Enkelmann and M. Baumgarten, *J. Phys. Org. Chem.*, 2006, **19**, 257–262; (*d*) C. Rajadurai, V. Enkelmann, G. Zoppellaro and M. Baumgarten, *J. Phys. Chem. B*, 2007, **111**, 4327; (*e*) C. Rajadurai, V. Enkelmann, V. Ikorskii, V. I. Ovcharenko and M. Baumgarten, *Inorg. Chem.*, 2006, **45**, 9664; (*f*) C. Rajadurai, K. Falk, S. Ostrovsky, V. Enkelmann, W. Haase and M. Baumgarten, *Inorg. Chim. Acta*, 2005, **358**, 3391.

6 (*a*) G. Zoppellaro, A. Ivanova, V. Enkelmann, A. Geies and M. Baumgarten, *Polyhedron*, 2003, **22**, 2099–2110; (*b*) G. Zoppellaro, V. Enkelmann, A. Geies and M. Baumgarten, *Org. Lett.*, 2004, **6**, 4929–4932; (*c*) C. Stroh, P. Turek, P. Rabu and R. Ziessel, *Inorg. Chem.*, 2001, **40**, 5334; (*d*) C. Stroh and R. Ziessel, *Tetrahedron Lett.*, 1999, **40**, 4543–4596; (*e*) F. M. Romero, D. Luneau and R. Ziessel, *Chem. Commun.*, 1998, 551; (*f*) D. Luneau, F. M. Romero and R. Ziessel, *Inorg. Chem.*, 1998, **37**, 5078; (*g*) D. Shiomi, K. Ito, M. Nishizawa, K. Sato, T. Takui and K. Itoh, *Synth. Met.*, 1999, **103**, 2271; (*h*) K. Osanai, A. Okazawa, T. Nogami and T. Ishida, *J. Am. Chem. Soc.*, 2006, **43**, 14008–14009; (*i*) R. G. Hicks, M. T. Lemaire, L. K. Thompson and T. M. Barclay, *J. Am. Chem. Soc.*, 2000, **122**, 8077; (*j*) T. M. Barclay, R. G. Hicks, M. T. Lemaire and L. K. Thompson, *Chem. Commun.*, 2000, 2141; (*k*) S. Fokin, V. Ovcharenko, G. Romanenko and V. Ikorskii, *Inorg. Chem.*, 2004, **43**, 969; (*l*) H. Oshio, T. Yaginuma and T. Ito, *Inorg.Chem.*, 1999, **38**, 2750.

7 (*a*) P. Gutlich and H. A. Goodwin, Spin crossover in transition metal compounds, in *Topics in Current Chemistry*, ed. Springer, Berlin, 2004, Vol. 233; (*b*) N. Chandrasekhar and R. Chandrasekar, *Dalton Trans.*, 2010, **39**, 9872–9878; (*c*) C. Rajadurai, Z. Qu, O. Fuhr, B. Gopalan, R. Kruk, M. Ghafari and M. Ruben, *Dalton Trans.*, 2007, **32**, 3531; (*d*) C. Rajadurai, O. Fuhr, R. Kruk, M. Ghafari, H. Hahn and M. Ruben, *Chem. Commun.*, 2007, 2636–2638; (*e*) C. Rajadurai, F. Schramm, S. Brink, O. Fuhr, R. Kruk, M. Ghafari and M. Ruben, *Inorg. Chem.*, 2006, **45**, 10019; (*f*) J. M. Holland, J. A. McAllister, Z. Lu, C. A. Kilner, M. Thornton-Pett and M. A. Halcrow, *Chem. Commun.*, 2001, 577.

8 (*a*) T. Ishida and H. Iwamura, *J. Am. Chem. Soc.*, 1991, **113**, 4238; (*b*) F. Kanno, K. Inoue, N. Koga and H. Iwamura, *J. Phys. Chem.*, 1997, **97**, 13267; (*c*) K. Inoue and H. Iwamura, *J. Am. Chem. Soc.*, 1994, **116**, 3173; (*d*) K. Inoue and H. Iwamura, *Adv. Mater.*, 1996, **8**, 73; (*e*) W. T. Borden, H. Iwamura and J. A. Berson, *Acc. Chem. Res.*, 1994, **27**, 109; (*f*) W. T. Borden and E. R. Davidson, *J. Am. Chem. Soc.*, 1977, **99**, 4587.

9 J. H. Osiecki and E. F. Ullman, *J. Am. Chem. Soc.*, 1968, **90**, 1078.

10 C. Hirel, K. E. Vostrikova, J. Pècaut, V. I. Ovcharenko and P. Rey, *Chem.–Eur. J.*, 2001, **7**, 2008.

11 WINEPR-SIMfonia programme was used for the simulation of the experimental ESR spectra.

